

# Theory of Manganites Exhibiting Colossal Magnetoresistance

T. V. Ramakrishnan<sup>\*†</sup>, H. R. Krishnamurthy<sup>\*†</sup>,  
S. R. Hassan<sup>\*†</sup> and G. Venketeswara Pai<sup>\*‡</sup>

June 4, 2018

<sup>\*</sup>Centre for Condensed Matter Theory, Department of Physics, Indian Institute of Science, Bangalore-560012, India

<sup>†</sup>Condensed Matter Theory Unit, Jawaharlal Nehru Centre for Advanced Scientific Research, Jakkur P.O , Bangalore-560064, India

<sup>‡</sup>The Abdus Salam International Centre for Theoretical Physics, 11 Strada Costiera, Trieste 34014, Italy

## Abstract

The electronic properties of many transition metal oxide systems require new ideas concerning the behaviour of electrons in solids for their explanation. A recent example, subsequent to that of cuprate superconductors, is of rare earth manganites doped with alkaline earths, namely  $Re_{1-x}A_xMnO_3$ , which exhibit colossal magnetoresistance, metal insulator transition and many other poorly understood phenomena. Here we show that the strong Jahn Teller coupling between the twofold degenerate ( $d_{x^2-y^2}$  and  $d_{3z^2-r^2}$ )  $e_g$  orbitals of  $Mn$  and lattice modes of vibration (of the oxygen octahedra surrounding the  $Mn$  ions) dynamically reorganizes the former into a set of states (which we label  $\ell$ ) which are localized with large local lattice distortion and exponentially small intersite overlap, and another set (labelled  $b$ ) which form a broad band. This hitherto unsuspected but microscopically inevitable *coexistence* of radically different  $\ell$  and  $b$  states, and their relative energies and occupation as influenced by doping  $x$ , temperature  $T$ , local Coulomb repulsion  $U$  etc., underlies the unique effects seen in manganites. We present results from strong correlation calculations using the dynamical mean-field theory which accord with a variety of observations in the orbital liquid regime (say, for  $0.2 \lesssim x \lesssim 0.5$ ). We outline

extensions to include intersite  $\ell$  coherence and spatial correlations/long range order.

## 1 Introduction

Solid state oxides containing transition metal ions with unfilled  $d$  shell electrons have been at the centre of attention in condensed matter and materials physics for the last two decades because of the variety and novelty of electronic phenomena in them and the possibility of new applications. The  $d$  electrons in solids are not as extended as  $s, p$  electrons or as localized as  $f$  electrons. Their motion in the system is highly constrained by the large local (on site)  $d - d$  repulsion or Mott-Hubbard correlation  $U$ . The central question is how this strong correlation, and other factors such as orbital degeneracy and electron lattice coupling, lead to electronic behaviour qualitatively different from that of conventional solids which are successfully described as degenerate Fermi liquids with well defined interacting electronic quasi-particles.

While the best known examples of these are the high  $T_c$  cuprate superconductors [1], during the last decade another group of oxides, namely the manganites  $Re_{1-x}A_xMnO_3$  (where  $Re = La, Pr, Nd$  etc. and  $A = Ca, Sr, Ba$  etc.) has become a focus of major activity. The initial interest was sparked by the discovery [2] that their electrical resistivity changes enormously with the application of a magnetic field, the change (colossal magnetoresistance or CMR) being two or more orders of magnitude larger than the normal cyclotron orbital effect characterized by the dimensionless parameter  $(\omega_c\tau)^2$ . Subsequent work has shown a bewildering variety of phases, phase transitions and phenomena [3, 4] depending on the doping  $x$ , temperature  $T$ , and ionic species  $Re$  and  $A$  as well as external perturbations. An example is the phase diagram of  $La_{1-x}Ca_xMnO_3$  (Fig. 1) which shows an insulating,  $Mn - O$  bond (Jahn-Teller) distorted but structurally ordered phase for small  $x$ , the transition of this at low  $T$  from a ferromagnetic insulator to a ferromagnetic metal at  $x \simeq 0.2$ , and thence to a charge ordered insulating phase for  $x \gtrsim 0.5$ . For  $0.2 \lesssim x \lesssim 0.5$  this becomes a paramagnetic insulator above a  $T_c \gtrsim 250 K$ , with CMR near  $T_c$ . The phase diagram varies considerably with the ionic species. For example,  $La_{1-x}Sr_xMnO_3$  has a paramagnetic metallic phase for  $0.175 \lesssim x \lesssim 0.5$  and shows no charge/orbital order, while  $Pr_{1-x}Ca_xMnO_3$  has no metallic phases (even ferromagnetic)[3, 4]. Two other general characteristics are the following. First, physical properties are extremely sensitive to small perturbations; examples being the CMR itself, the unusually large strain and ion size effects [5, 6, 7], the melting of charge/orbital ordering for anomalously small magnetic fields and a metal to insulator transition induced by the electronically be-

nign substitution of  $O^{16}$  by  $O^{18}$  [8]. Secondly, over a wide range of  $x$  and  $T$ , two very different types of regions, one insulating and locally lattice distorted and the other metallic and undistorted, coexist [9]. The regions can be static [10, 11] or dynamic [11, 12, 13]; their size can vary from  $100 \text{ \AA}$  [14] to  $3000 \text{ \AA}$  [10]. All these observations suggest that metallic and insulating phases are always very close in free energy.

These phenomena cannot be described satisfactorily in terms of well known models for electrons in solids. For example, one might expect generally that doping  $LaMnO_3$  (a Mott insulator) with  $Ca$  introduces mobile holes in the  $Mn - d$  band so that the system ought to be metallic at least in the high symmetry paramagnetic phase; but it is not till  $x \simeq 0.20$ . The observed properties of manganites need to be understood in terms of the active degrees of freedom which are believed to be the twofold degenerate  $e_g$  electrons and the  $t_{2g}$  core-spins of  $Mn$ , and Jahn-Teller(JT) optical phonon modes of the oxygen octahedra and the interactions between them. There are three strong interactions present, namely the large on site  $d - d$  repulsion  $U \simeq 5 eV$  [15, 16] amongst the  $e_g$  electrons, strong JT mode -  $e_g$  electron coupling  $g$  which splits the doubly degenerate  $e_g$  level by about  $2E_{JT} \simeq 1 eV$  [17, 18], and the large ferromagnetic Hund's rule coupling  $J_H$  between  $e_g$  and  $t_{2g}$  spins ( $\simeq 1$  to  $2 eV$  [15, 16]). For comparison, the  $e_g$  electron kinetic energy scale or band width  $W \equiv 2D_o$  is  $\simeq 2 eV$  [15, 16]. The presence of a large JT coupling is clearly indicated by the two 'phase' coexistence[9] (with one 'phase' being lattice distorted and insulating, and the other metallic and undistorted) as well as by the sensitivity of properties to lattice strain or local disorder, and giant isotope effect[8, 19] alluded to above. Indeed, large JT distortions, while long ranged in  $LaMnO_3$ , persist locally well into the metallic regime[11, 12] ( $x \lesssim 0.3$ , and  $T \gtrsim 77 K$ ), where they are short ranged. Understanding the observed consequences of these interactions is one of the major challenges in the physics of strongly correlated electrons.

Most existing theories [20, 21, 22, 23, 9] for manganites neglect one or the other of these strong interactions, make further approximations, and are inadequate qualitatively and quantitatively. The earliest theoretical approaches [20], commonly referred to as double exchange theories, consider solely the Hund's rule exchange  $J_H$ . However, only a metallic state is possible in this case. A theory due to Millis, Mueller and Shraiman [21] additionally includes the effect of the coupling  $g$ , but treats the local JT lattice distortion classically, as annealed static disorder, and neglects  $U$ . A polaronic insulating phase also occurs in that case for large enough  $g$ , but the predicted results do not resemble experiments; for example at  $x \neq 0$ , one finds only metal-metal or insulator-insulator Curie transitions, unlike the commonly observed metal-insulator transition. The magnetoresistance is not colossal and there is no iso-

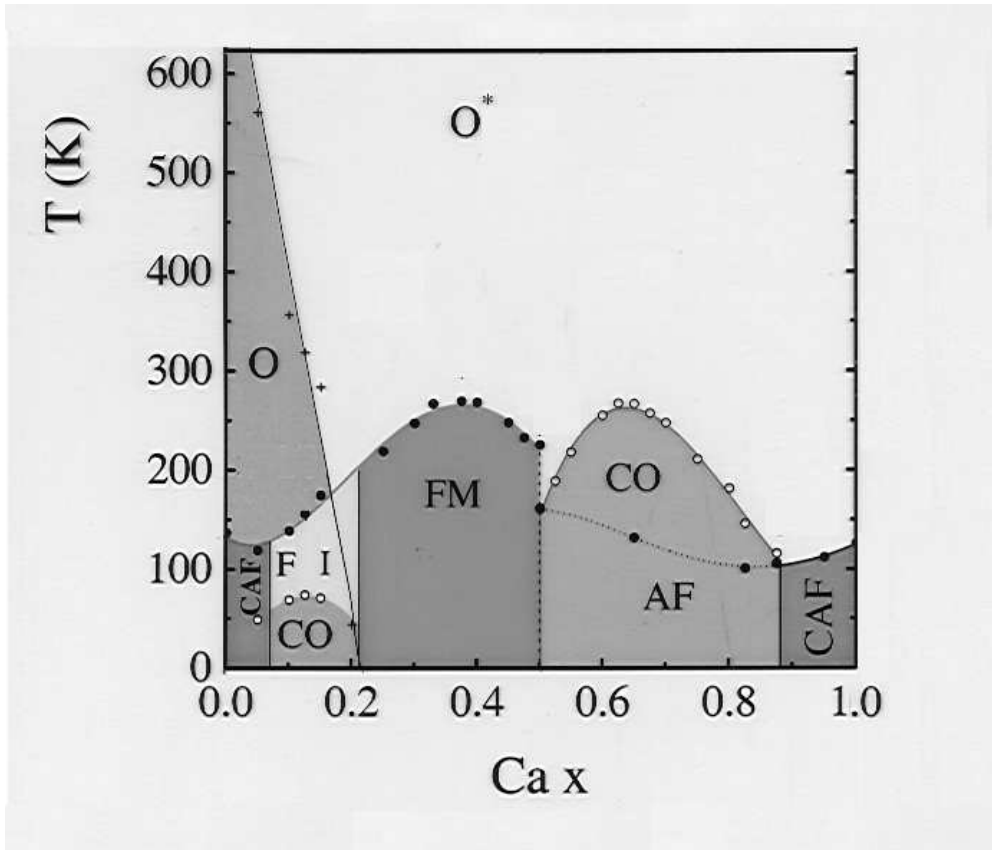


Figure 1: The phase diagram of  $La_{1-x}Ca_xMnO_3$  in the doping  $x$  and temperature  $T$  plane (adapted from Ref. [24]). Various kinds of anti-ferromagnetic insulator(AF), paramagnetic insulator(PI), ferromagnetic insulator(FI), ferromagnetic metal(FM) and charge/orbitally ordered insulator(CO/O  $O^*$ ) are the phases shown.  $O$  and  $O^*$  are Orthorhombic(Jahn-Teller distorted) and Orthorhombic(Octahedron rotated) structural phases.

tope effect. Dagotto and coworkers (see eg. Ref. [9]) have done extensive numerical simulations of several models, but on rather small lattices, and seen lots of instances of "phase separation". The early simulations explored the competition between (double exchange induced) ferromagnetism and anti-ferromagnetic (super)exchange, amplification and generation of small scale phase co-existence by disorder, and identified the two kinds of magnetic domains with metallic and insulating regions. Later simulations explored similar issues including static JT couplings. Based on these, they suggest[9] that transport in manganites should be pictured in terms of a random resistor network arising from tunnelling between misaligned ferromagnetic metallic domains across insulating regions, and that the CMR arises from enhanced tunnelling due to field induced alignment of the magnetic domains. There are many other models designed to address specific effects, but no theoretical ideas which explain the novel general features of manganites cohesively.

We propose here a new approach to the physics of manganites which includes all the three strong interactions, the double degeneracy of  $e_g$  orbitals as well as the quantum dynamics of phonons. It leads to a simple physical description from which the properties of manganites follow naturally. Calculations of ground state and transport properties at finite temperatures are also presented. We believe that the ideas are of wide relevance to a large number of solid state and molecular systems with similar ingredients.

## 2 Coexisting polaronic and band states

Our ideas are principally based on two facts; namely the two fold degeneracy of the  $e_g$  orbital and the strong (degeneracy lifting) JT interaction characterized by the large dimensionless ratio ( $E_{JT}/\hbar\omega_0$ ), ( $\simeq 10$  for manganites, see ref.[17]) where  $\hbar\omega_0$  is the JT optical phonon energy  $\simeq 0.075 eV$  [25]. This coupling leads (as shown in greater detail below) to a large local JT distortion  $Q_0$  being associated with one linear combination of the orbitals (JT polaron, labelled  $\ell$  by us) when it occupied by a single electron. If the JT modes are not approximated as static displacements [21] but are treated quantum-dynamically, the inter-site hopping of the JT polaron is reduced by the exponential Huang Rhys [26] factor  $\eta \equiv \exp\{-(E_{JT}/2\hbar\omega_0)\} \simeq (1/200)$  for  $E_{JT} = 0.6 eV$  and  $\hbar\omega_0 \simeq 0.06 eV$ . This is the *antiadiabatic limit* overlap between the initial and final JT phonon wave functions (centred around  $Q_0$  and 0) when the  $\ell$  electron moves in or out of a site. The corresponding effective  $\ell$ -bandwidth,  $W^* \equiv k_B T^* \simeq W\eta \simeq k_B(125 K)$ , is thus very small, so the  $\ell$  states are easily localized by any disorder present (eg. in cation site energy). They can hence be

regarded, to a first approximation (which may be inaccurate for  $T < T^*$  because of inter-site coherence, see Section 8), as non dispersive localized levels. The  $\ell$  polaron is probably close to this limit over a wide range of  $x$  and  $T$ , where large local  $JT$  distortion without long range order is seen [11, 12].

Since the  $e_g$  orbital at each site is doubly degenerate initially, there is another orthogonal set of states which we label  $b$ , which have their largest amplitudes at the fraction  $x$  of hole sites where the polaron is not present; their occupancy on the polaron site costs a large extra energy  $\bar{U} = (U + 2E_{JT})$ . The (bare) hopping  $\bar{t}$  amongst these  $b$  states is not reduced and they form a broad band (of bare width  $2D_o \simeq 2$  eV ) whose properties are strongly affected, eg. their effective bandwidth  $2D$  is renormalized to smaller values, by the other two strong interactions present in the system, namely the repulsive scattering from the  $\ell$  polarons ( $\bar{U}$ ) and the coupling to the  $t_{2g}$  spins ( $J_H$ ) depending on  $x$  and  $T$ . Roughly,  $2D$  increases with  $x$  as well as with  $T^{-1}$  and  $H$ , because the inhibition of  $b$  hopping due to large  $\bar{U}$  is reduced when there are more hole-sites, and that due to large  $J_H$  is reduced when the  $t_{2g}$  spin order is enhanced.

We believe that the unique feature of manganites is this necessary coexistence of antiadiabatic,  $JT$  distorted, localized ( $\ell$ ) states and adiabatic, undistorted, broad band ( $b$ ) states, arising from a *spontaneous reorganization of the doubly degenerate  $e_g$  states due to the large  $JT$  coupling and quantum phonon dynamics*. This dynamically generated coexistence is qualitatively different from that of localized  $f$  and extended  $s, p, d$  electrons in rare earth solids, which has an atomic origin. We show below that for a wide range of  $x$  and  $T$ , both sets of states are partially occupied. This, we believe, underlies the ubiquitous two ‘phase’ coexistence observed [9]. The high sensitivity of the physical properties of manganites to small perturbations arises because the ( $\ell$ ) states, being localized and lattice distorted, are strongly influenced by local perturbations, which then affects the delicate relative stability of  $\ell$  and  $b$  states.

Finally, (again as discussed in more detail below,) the existence of the localized polaronic  $\ell$  states *in the presence of large  $U$  and  $J_H$*  give rise to a *new, major, doping dependent ferromagnetic nearest neighbour exchange coupling  $J_F$*  between the  $t_{2g}$  core spins. This comes about due to *virtual, fast (adiabatic) hopping processes* of the  $\ell$  electrons to neighbouring empty sites and back, leading to a  $J_F$  roughly of order  $x(1-x)\bar{t}^2/(2E_{JT}S^2)$ , the intermediate state energy due to the unrelaxed lattice distortion being  $2E_{JT}$ . We get  $J_F \simeq 2meV$  for  $x = 0.3$ . Our calculations suggest that this *virtual, correlated double exchange due to the localized  $\ell$  electrons*, and not conventional double exchange due to mobile  $e_g$  electrons as hitherto believed, is the dominant source of ferromagnetism and of the ferromagnetic transition temperature  $T_c$  in the hole doped manganites.

### 3 A new model Hamiltonian for manganites in the strong electron lattice JT coupling regime

Based on the above ideas, and for the purposes of making quantitative calculations and predictions, we have proposed[27, 28] a new model Hamiltonian for manganites given by

$$\begin{aligned}
 H_{lb} = & \sum_{i,\sigma} -(E_{JT} + \mu)\ell_{i\sigma}^+\ell_{i\sigma} - \mu \sum_{i,\sigma} b_{i\sigma}^+b_{i\sigma} \\
 & - \bar{t} \sum_{\langle ij \rangle, \sigma} b_{i\sigma}^+b_{j\sigma} + U \sum_{i,\sigma} n_{\ell i\sigma}n_{b i\sigma} + H_s
 \end{aligned} \tag{1}$$

Here  $\ell_{i\sigma}^+$  creates the JT polaronic state of energy  $-E_{JT}$  and spin  $\sigma$ , localized at site  $i$  ( $\ell_{i\sigma}$  is the corresponding destruction operator). The broad band electron, created by the operator  $b_{i\sigma}^+$ , has mean energy zero, and nearest neighbour effective hopping amplitude  $\bar{t}$ . The two repel each other on site with energy  $U$ . The common chemical potential  $\mu$  is determined by the constraint that the filling, i.e., the average number of  $e_g$  electrons per site must be determined by the doping  $x$  according to

$$N^{-1} \sum_i \langle n_i \rangle \equiv N^{-1} \sum_i \sum_{\sigma} (\langle n_{\ell i\sigma} \rangle + \langle n_{b i\sigma} \rangle) = (1 - x). \tag{2}$$

The term  $H_s$  in Eq. 2 models the spin dependent interactions, and is given by

$$H_s = -J_H \sum_i \vec{s}_i \cdot \vec{S}_i - J_F \sum_{\langle ij \rangle} \vec{S}_i \cdot \vec{S}_j - \mu_B \sum_i \vec{S}_i \cdot \vec{h} \tag{3}$$

It includes the strong ferromagnetic Hund's rule coupling  $J_H$  between the  $e_g$  spins  $\vec{s}_i$  ( $\equiv (\vec{s}_{\ell i} + \vec{s}_{b i})$ ) and the (spin  $S = \frac{3}{2}$ )  $t_{2g}$  spins  $\vec{S}_i$ , the net effective ferromagnetic exchange coupling  $J_F$  between these  $t_{2g}$  spins (from the mechanism alluded to above, and discussed in more detail below), and the interaction of the latter with an external magnetic field  $\vec{H}$  [29]. For simplicity, in what follows we further approximate the  $t_{2g}$  spins as classical fixed length spins whose directions fluctuate, i.e. write  $\vec{S}_i = S\hat{\Omega}_i$  where  $\hat{\Omega}_i$  is a unit vector.

We now discuss how the above model Hamiltonian can be motivated from the microscopic Hamiltonian for the manganites in the limit of strong JT interaction. A reasonably realistic microscopic model Hamiltonian or energy operator  $H$  of  $d$  electrons ( $e_g$  and  $t_{2g}$ ) in the manganites has three types of contributions, namely those involving only the  $e_g$  electrons ( $H_e$ ), the coupling of these electrons with the

JT lattice modes as well as the energy of these lattice modes themselves ( $H_{el}$ ), and the part  $H_s$  which involves the  $e_g$  and  $t_{2g}$  spins. Thus

$$H = H_e + H_{el} + H_s \quad (4)$$

where

$$\begin{aligned} H_e &= \sum_{i,\sigma} (\epsilon_i - \mu) \tilde{n}_{i\sigma} + \sum_{\langle ij \rangle} \tilde{a}_{i\sigma}^+ \tilde{t}_{ij} \tilde{a}_{j\sigma}^+ \\ &+ U \sum_{i,\sigma\sigma'} (\tilde{n}_{i\sigma} \tilde{n}_{i\sigma'} - \tilde{n}_{i\sigma}) \end{aligned} \quad (5)$$

$$\begin{aligned} H_{el} \equiv \sum_i (H_{JT}^i + H_l^i) &= g \sum_{i,\sigma} \left( \tilde{a}_{i\sigma}^+ \tau^z \tilde{a}_{i\sigma} Q_{3i} + \tilde{a}_{i\sigma}^+ \tau^x \tilde{a}_{i\sigma} Q_{2i} \right) \\ &+ \frac{K}{2} \sum_i (Q_{2i}^2 + Q_{3i}^2) + \frac{1}{2M} \sum_i (p_{2i}^2 + p_{3i}^2) \end{aligned} \quad (6)$$

Here the operators  $\tilde{a}_{i\sigma}^+, \tilde{a}_{i\sigma}$  respectively add and remove an electron at site  $i$ , in the spin state  $\sigma$  which can take two values, and in the two  $e_g$  orbital states with labels  $\alpha = 1$  corresponding to  $d_{3z^2-r^2}$  and  $\alpha = 2$  corresponding to  $d_{x^2-y^2}$ ; i.e.,  $\tilde{a}_{i\sigma}^+$  is a short hand for  $(a_{i1\sigma}^+, a_{i2\sigma}^+)$ . The number operator  $\tilde{n}_{i\sigma}$  is the usual sum  $\sum_{\alpha} a_{i\alpha\sigma}^+ a_{i\alpha\sigma} \equiv \tilde{a}_{i\sigma}^+ \tilde{a}_{i\sigma}$ . The  $e_g$  electron has site energy  $\epsilon_i$ , equal to 0 for a clean system. The (anisotropic and orbital dependent) nearest neighbour hopping *matrix* is  $\tilde{t}_{ij}$  and  $U$  is the repulsion between electrons at  $i$  in different states. The first set of terms in  $H_{el}$  describes the coupling of  $e_g$  electrons with the two JT lattice modes  $Q_{3i}$  and  $Q_{2i}$  with strength  $g$ , ( $\tau^a$  being the usual Pauli matrices in orbital space) the former displacement leading to a splitting and the latter to a mixing of the two  $e_g$  states. The last two terms in  $H_{el}$  are the potential and kinetic energies of the modes neglecting anharmonic and intersite terms.  $H_s$  is the same magnetic Hamiltonian as in eqn. 3 (except that, in the context of the microscopic hamiltonian, the  $e_g$  spin  $\vec{s}_i \equiv \frac{1}{2} \sum_{\mu\mu'} \tilde{a}_{i\mu}^+(\vec{\sigma})_{\mu\mu'} \tilde{a}_{i\mu'}$  where  $\vec{\sigma}$  is the Pauli spin operator).

In manganites the JT coupling  $g$  is large compared to  $t/Q_0$  (where  $Q_0$  is the typical size of the JT distortion), and one can first concentrate on the single site, coupled electron-phonon problem. The Schrodinger equation corresponding to  $H_{JT}^i + H_l^i$  can be solved exactly at a single site.  $\vec{Q}_i \equiv (Q_{2i}, Q_{3i})$  is like a local pseudo-magnetic field splitting the pseudo-spin 1/2 orbital levels 1 and 2, hence  $H_{JT}^i$  has eigenvalues  $\pm gQ_i$ , where  $Q_i = |\vec{Q}_i|$  is the magnitude of the JT distortion. The diagonalization of  $H_{JT}^i$  can be done explicitly using the operators

$$b_i^+ \equiv \cos(\theta_i/2) a_{i1}^+ + \sin(\theta_i/2) a_{i2}^+ \quad (7)$$



and

$$\tilde{\ell}_i^+ \equiv -\sin(\theta_i/2)a_{i1}^+ + \cos(\theta_i/2)a_{i2}^+, \quad (8)$$

where  $\theta_i \equiv \tan^{-1}(Q_{2i}/Q_{3i})$ , i.e., it determines the orientation of the JT distortion. When an electron is present at site  $i$  in the  $\tilde{\ell}$  state, the effective lattice potential energy at site  $i$  in  $H_{JT}^i + H_i^i$  has the form

$$V_i^- = (KQ_i^2/2 - gQ_i) \quad (9)$$

This has a minimum at  $Q_0 = (g/K)$  (the JT polaronic distortion) with an energy lowering of  $E_{JT} = (g^2/2K) \sim .5$  eV independent of  $\theta_i$  [30]. The JT polaronic  $\ell$  state that we referred to above is this  $\tilde{\ell}$  state *together with the JT distortion*. When an electron is present in the other ‘anti’ JT,  $b$  state, the effective lattice potential energy is

$$V_i^+ = (KQ_i^2/2 + gQ_i) \quad (10)$$

with a minimum at zero displacement so that no distortion is associated with it.

Thus, when an  $\ell$  polaron is present at a site, low energy lattice configurations around the deep minimum of  $V_i^-$  involve a shift of  $Q_i$  by an amount  $Q_0$  at each site. This is formally achieved by a Lang-Firsov transformation [31]  $\hat{\eta}_i \equiv \exp\{-(ip_i Q_0/\hbar)\}$  where  $p_i$  is the radial momentum operator conjugate to  $Q_i$ . In other words, formally, one has  $\ell_i^+ \equiv \hat{\eta}_i \tilde{\ell}_i^+$ . The Huang-Rhys reduction factor [26]  $\eta \equiv \exp\{-(E_{JT}/2\hbar\omega_0)\}$  we have alluded to earlier, which multiplies the hopping involving the  $\ell$  states, is just the ground state expectation value of  $\hat{\eta}_i$ , corresponding to the anti-adiabatic limit overlap of the distorted phonon wavefunction at a site with the undistorted phonon wavefunction. (We ignore fluctuations on the basis that  $\bar{t}\eta \ll \hbar\omega_0$  [32]). The coherent intersite hopping of the  $\ell$  electrons is thus  $t^* = \bar{t}\eta \simeq 10K$ , very small, and can be neglected to a first approximation. The ‘anti’ Jahn Teller state  $b$  has no associated lattice distortion, so its hopping amplitude  $t_{ij}$  is not reduced, but depends on the angles  $\theta_i$  and  $\theta_j$  at sites  $i$  and  $j$ . We assume a nearest neighbour hopping amplitude  $\bar{t}_{ij} = \bar{t}$  averaged over angles  $\theta_i$  either statistically (and classically) or by quantum fluctuations. Such an *orbital liquid* approximation is reasonable for the phases with no long range orbital order, i.e., for  $0.2 \lesssim x \lesssim 0.5$  in most manganites, but poor for those other values of  $x$  for which one has strong orbital correlations or long range orbital order.

The localized polaronic  $\ell$  and the broad band  $b$  states coexist in manganites since the conditions for anti-adiabaticity of the former, namely  $\bar{t}\eta \ll \hbar\omega_0$  and the adiabaticity of the latter, namely  $\bar{t} \gg \hbar\omega_0$ , are *both* fulfilled. The  $b$  electrons are repelled strongly by the  $\ell$  electrons, with energy  $\bar{U} = U + 2E_{JT}$ , and hence will have

the largest amplitudes at sites where the  $\ell$  electrons are not present, i.e. at the hole sites. They hop quickly (time scale  $\hbar/\bar{t} \ll 1/\omega_0$ ) among such sites, avoiding strongly the sites with static  $\ell$  electrons, where they hence have small amplitudes[33].

Finally we discuss the result alluded to above namely that the existence of localized, JT distorted  $\ell$  states in the presence of large  $J_H$  and large  $U$  can give rise to a new mechanism of ferromagnetic exchange between the  $t_{2g}$  core spins, which we refer to as "virtual double exchange".

Suppose that a localized  $\ell$  electron is present at a site, and that site is distorted. The  $\ell$  electron can take part in fast (adiabatic) virtual hopping processes to neighbouring sites, i.e., leaving the local lattice distortion unrelaxed, by paying an energy cost of  $2E_{JT}$  in the intermediate state. For large  $U$  this can happen only if the neighboring state is empty, and for large  $J_H$  only if the  $t_{2g}$  spins on the two sites are parallel. (Otherwise the energy of the intermediate state will increase by  $U$  and  $J_H$  respectively.) Clearly, from second order perturbation theory this process will give rise to a *new,  $\ell$  occupancy dependent, ferromagnetic exchange coupling* between the  $t_{2g}$  core spins of the form

$$\left(\frac{\bar{t}^2}{2E_{JT}}\right) \frac{1}{2}(\hat{\Omega}_i \cdot \hat{\Omega}_j + 1)[n_{\ell i}(1 - n_j) + n_{\ell j}(1 - n_i)] \quad (11)$$

(where we have again ignored the dependence on the angles  $\theta_i$  etc). The  $\frac{1}{2}(\hat{\Omega}_i \cdot \hat{\Omega}_j + 1)$  factor comes from large  $J_H$ , and the occupancy dependent terms from large  $\bar{U}$ . Within the homogeneous orbital liquid approximation we are using in this paper, this translates to an effective ferromagnetic interaction proportional to  $x\bar{n}_\ell \simeq x(1 - x)$  as stated earlier.

The normal super-exchange coupling between  $t_{2g}$  core spins on neighboring sites is of order  $\bar{t}^2/U$ , and its sign depends on the nearest neighbour orbital correlations [34]. For example, in  $LaMnO_3$  it is anti-ferromagnetic along the c axis, and ferromagnetic in plane. Conventional double exchange can, in principle, explain metallic ferromagnetism in the manganites, but would be unable to account for ferromagnetism in their insulating phases in the absence of orbital correlations. The above mechanism yields a ferromagnetic coupling which is clearly much larger than and dominates the super-exchange for all intermediate doping, operates even in the insulating states and even in the orbital liquid phase, and as we discuss later, makes the dominant contribution to the ferromagnetic  $T_c$  even in the metallic case.

Putting all this together, expressing the on site coulomb and exchange interactions in the  $\ell$  and  $b$  basis, and including the new exchange mechanism, leads us to the suggestion that in the large  $(E_{JT}/\hbar\omega_o)$  limit, and for describing low energy electronic

properties the microscopic model Hamiltonian in Eq. 4 can be approximated by the much simpler, two fermion species, Hamiltonian  $H_{\ell b}$  given in Eq. 2. The relatively small  $g\mu_B\vec{H} \cdot \vec{s}_i$  term and other coulomb repulsion terms (between  $\ell$  and  $b$  electrons of different spins) have been neglected in  $H_{\ell b}$  because of the large  $J_H$  ( $J_H \gg \bar{t}$ ) limit of relevance here (whence the spin of the  $\ell$  and  $b$  electrons is forced to be parallel to the  $t_{2g}$  spin), and we have relabelled the effective repulsion between the two types of electrons as  $U$ .

## 4 DMFT wth polaronic and band states

Apart from the constraint equation Eq. 2 and the spin dependent  $H_s$ ,  $H_{\ell b}$  is essentially the well known Falicov-Kimball model (FKM)[35] for non hybridizing  $f$  electrons in a broad band metal with correlations. Indeed at  $T = 0$ , in the ferromagnetic phase and for large  $J_H$ , the spin degrees of freedom are completely frozen, whence it reduces to the (spin-less) FKM. More generally, it describes the dynamics of the  $b$  electrons moving in an *annealed disordered* background of immobile  $\ell$  electrons and  $t_{2g}$  spins in the presence of strong on site repulsion  $U$  and Hund's coupling  $J_H$ , the annealed disorder distribution being *thermodynamically and self-consistently determined*. This strong correlation problem cannot be solved in general, but can be solved within the framework of dynamical mean field theory (DMFT) [36] which is exact at  $d = \infty$ , and is quite accurate for three dimensions. We have carried out these DMFT calculations for thermodynamic properties (the occupancies  $\bar{n}_\ell$ ,  $\bar{n}_b$ , the magnetization  $m \equiv \langle \vec{S}_i \rangle$ , the specific heat, magnetic susceptibility, etc.), spectral behaviour (eg. the  $b$  band self-energy, propagator and density of states(DOS)) and transport (resistivity and magnetoresistance). While the specific results we discuss below come from such calculations, we believe that many of the physical mechanisms that underlie the results have a larger sphere of validity.

The properties of  $H_{\ell b}$  are determined largely by the dynamics of the  $b$  electrons, eg., their propagator or Green's function  $G_{ij}(\omega)$ , as affected by the (annealed disordered) distribution of  $n_{\ell i}$  and  $\hat{\Omega}_i$  due to strong  $U$  and  $J_H$ . In the DMFT framework, the  $b$  electron self energy  $\Sigma_{ij}(\omega)$  due to these interactions is site local, i.e.  $\Sigma_{ij}(\omega) = \delta_{ij} \Sigma(\omega)$ , and is determined self consistently. The general approach is well known [36].

Essentially, the problem reduces to that of one site, with its local degrees of freedom and interactions, immersed in an effective medium (comprising the other sites). We make the simplest reasonable approximation corresponding to a homogeneous annealed system, namely that  $\langle n_{\ell i\sigma} \rangle \equiv \bar{n}_{\ell\sigma}$ ,  $\langle n_{b i\sigma} \rangle \equiv \bar{n}_{b\sigma}$  and  $\langle \hat{\Omega}_i \rangle \equiv \vec{m} = m\hat{z}$  are the

same at every site  $i$ , and that there are no correlations between these quantities at different sites[37]. Consistent with this, we approximate the ferromagnetic exchange interactions in  $H_s$  in terms of a homogeneous molecular field in the standard way and replace

$$H_s = -J_H S \sum_i \vec{s}_i \cdot \hat{\Omega}_i - (\vec{h} + \bar{J}_F \vec{m}) \cdot \sum_i \hat{\Omega}_i \quad (12)$$

Here  $\vec{h} \equiv g\mu_B S \vec{H}$ ,  $\bar{J}_F \equiv 2zJ_F S^2$  where  $z$  is the co-ordination number. The quantity  $m$ , proportional to the magnetization, and  $\bar{n}_{\ell\sigma}$ , the average occupancy of the polaronic states, are also to be determined self-consistently.

Thus, in the present context, the effective medium is a homogeneous electron bath with which the local  $b$  electron hybridizes, the molecular field  $\bar{J}_F m$  in Eq. 12, and the local distributions of  $n_{\ell\sigma}$  and  $\hat{\Omega}$ . The on-site  $b$  electron propagator due to the medium, but without the local interactions, is  $\mathcal{G}$  where the (Matsubara) frequency variable and the spin label are suppressed. The single site problem can be solved exactly, just as in the Falicov-Kimball case [36], to determine (1) the (homogeneous) annealed distributions  $P(n_\ell)$  and  $P(\hat{\Omega})$  as functionals of  $\mathcal{G}$ ,  $m$  and the model parameters and (2) the local  $b$  electron propagator  $G$  as a functional of  $\mathcal{G}$ ,  $m$ , the model parameters and these annealed distributions. There are two other formal relations among  $G$ ,  $\mathcal{G}$  and  $\Sigma$ , namely ( $G^{-1} = \mathcal{G}^{-1} - \Sigma$ ) and  $G = \sum_{\vec{k}} [(G_{\vec{k}}^{0-1} - \Sigma)^{-1}]$ . By iterating these equations to self-consistency, one can determine  $\Sigma$ ,  $G$ ,  $\mathcal{G}$ ,  $P(n_\ell)$  and  $P(\hat{\Omega})$  (and hence  $\bar{n}_{\ell\sigma}$ ,  $\bar{n}_{b\sigma}$  and  $m$ ) explicitly for any chosen values of the model parameters  $U$ ,  $\epsilon_\ell$ ,  $\bar{t}$  and  $\bar{J}_F$  at a fixed  $T$  and  $\mu$  (the latter being chosen such that  $\bar{n}_\ell + \bar{n}_b = (1-x)$ ). Thermal, spectral and transport properties can be calculated in a straightforward way [36] from the  $b$  electron propagator. For example, the current-current correlation function (the Kubo formula) which determines the electrical (and optical) conductivity, can be expressed entirely in terms of  $G_{ij}(\omega)$ , vertex corrections being negligible.

The resulting calculations, while straightforward, still involve extensive numerics. The calculations whose results are described below have been done in the large  $J_H$  limit, i.e. assuming that the spin of the  $\ell$  and  $b$  electrons are forced to be aligned along  $t_{2g}$  spin  $\vec{\Omega}$ , whence there is considerable simplification [21, 37]. We have done such calculations both for a realistic model  $\bar{t}$  and for a model semicircular density of states. The two results are not very different, and here we mostly discuss results for the latter case, which has the advantage that some exact analytical results can be obtained in the  $U = \infty$ ,  $T = 0$  limit, and even the finite  $U$ , non-zero  $T$  calculations are much simpler. The details are described in refs. [28, 27, 38] and other papers we will publish elsewhere.

## 5 Metal insulator transitions

To start with, we show how the ideas above lead to a simple physical understanding of insulator metal transitions (IMT) in manganites, based on the variation of the occupancies and relative energies of the  $\ell$  and  $b$  states with  $U, x, T$  etc.

Fig. 2 shows the density of states for  $(E_{JT}/D_o) = 0.5$ ,  $D_o = 1 eV$ ,  $U = \infty$  (and  $\bar{J}_F = 60.2 meV$ ) for several values of  $x$  at  $T = 0$ . At  $T = 0$ , because of  $J_F$  the ground state is ferromagnetic, and the spin degrees of freedom are completely frozen. For large  $U$ , the renormalized or effective  $b$  bandwidth  $D$  self consistently goes to zero as  $x \rightarrow 0$ , whence for small  $x$  the bottom of the  $b$  band will be above the  $\ell$  level (of energy  $-E_{JT}$ ) and all electrons are in the latter states, as in Fig. 2a. For, the low energy  $b$  band states are constrained to reside mostly on the small fraction  $x$  of empty, undistorted sites, and have a small amplitude at the lattice distorted sites (where  $\ell$  electrons are present) from which they are repelled with energy  $U$ . The system is hence an insulator. This cannot happen in a pure double exchange model, where ferromagnetism and metallicity go together. As  $x$  increases, so does  $D$ , and there is a critical  $x_c$  ( $= 0.25$  within DMFT for the parameters used in Fig.2) at which the  $b$  band bottom touches the  $\ell$  level energy as in Fig.2b. For  $x > x_c$ , the  $b$  band bottom goes below the  $\ell$  level, and some of the  $\ell$  electrons are transferred to the  $b$  band until all  $b$  levels up to the (now renormalized)  $\ell$  level are occupied as in Fig. 2c. The system is then a ferromagnetic metal, but most of the electrons (0.6 per site out of the 0.7 present) are in the polaronic  $\ell$  state though there is no long range JT order.

Thus there is an IMT, not at  $x = 0$  as in a naive doped Mott insulator picture, but at  $x_c \neq 0$ . This shift is due to the strong electron lattice coupling  $g$  which makes the JT polaronic  $\ell$  level possible and stabilizes it by an energy  $E_{JT}$ , and large  $U$ , which makes the  $b$  electron bandwidth vanish as  $x \rightarrow 0$ . For  $U \rightarrow \infty$ , within DMFT we can show[28] that  $D = D_o\sqrt{x}$  whence we obtain  $x_c$  analytically as  $x_c = (E_{JT}/D_o)^2$  where  $D_o$  is the bare half-width of the b-band. The decrease of  $x_c$  with increasing  $D_o$  and its numerical value for reasonable choices of  $E_{JT}$  and  $D_o$  are in accord with experiments (for example, as one goes from  $LaCaMnO_3$  to  $LaSrMnO_3$  which has a larger bandwidth). Finite  $U$  corrections to  $x_c$ , which we have calculated, are small for  $U \simeq 5eV$  which is appropriate to these systems. A more detailed discussion of these and other zero temperature results is presented in [28].

Fig.3 shows the evolution of the spectral functions with temperature, for parameter values that correspond to  $Sr$  doping, for a fixed doping of  $x = 0.175 > x_c$  for this system, and for the temperature values  $T = 100K, 180K, 208K, 300K$ . For  $x > x_c$ , the system is metallic so that both  $b$  and  $\ell$  electronic states occupied. On increasing the

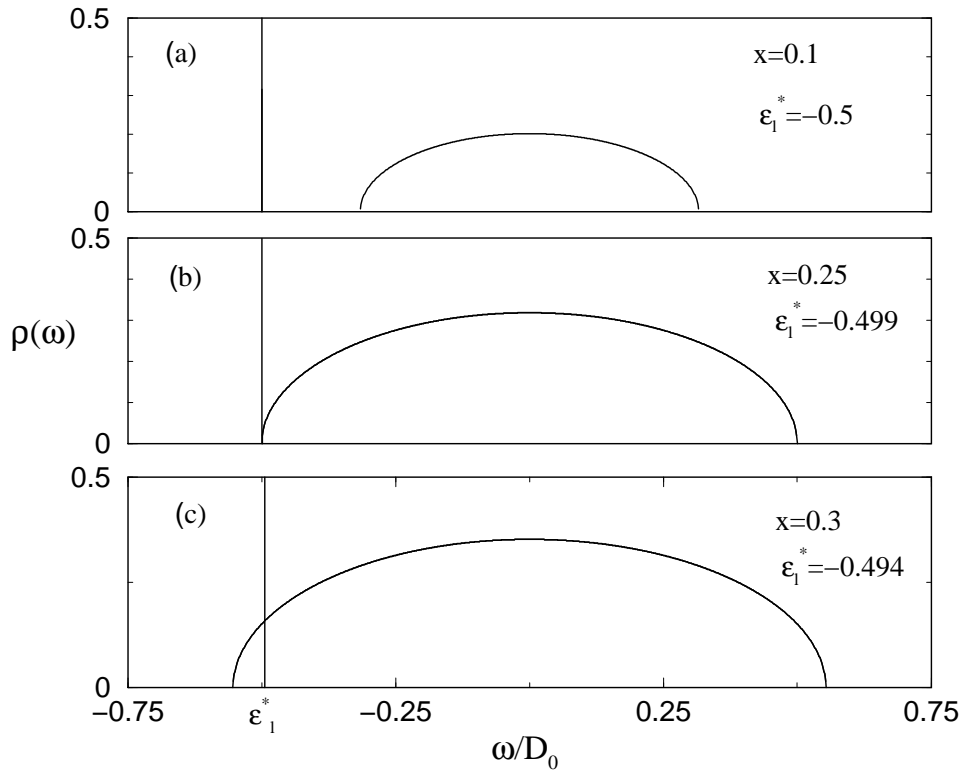


Figure 2: Evolution of DOS of the  $b$  band for various doping values of  $x = 0.1, 0.25, 0.3$  and  $T = 0$  with parameters  $E_{JT} = 0.5 eV$ ,  $D_o = 1 eV$ . The effective  $\ell$  level, labelled as  $\epsilon_\ell^*$  is also indicated.

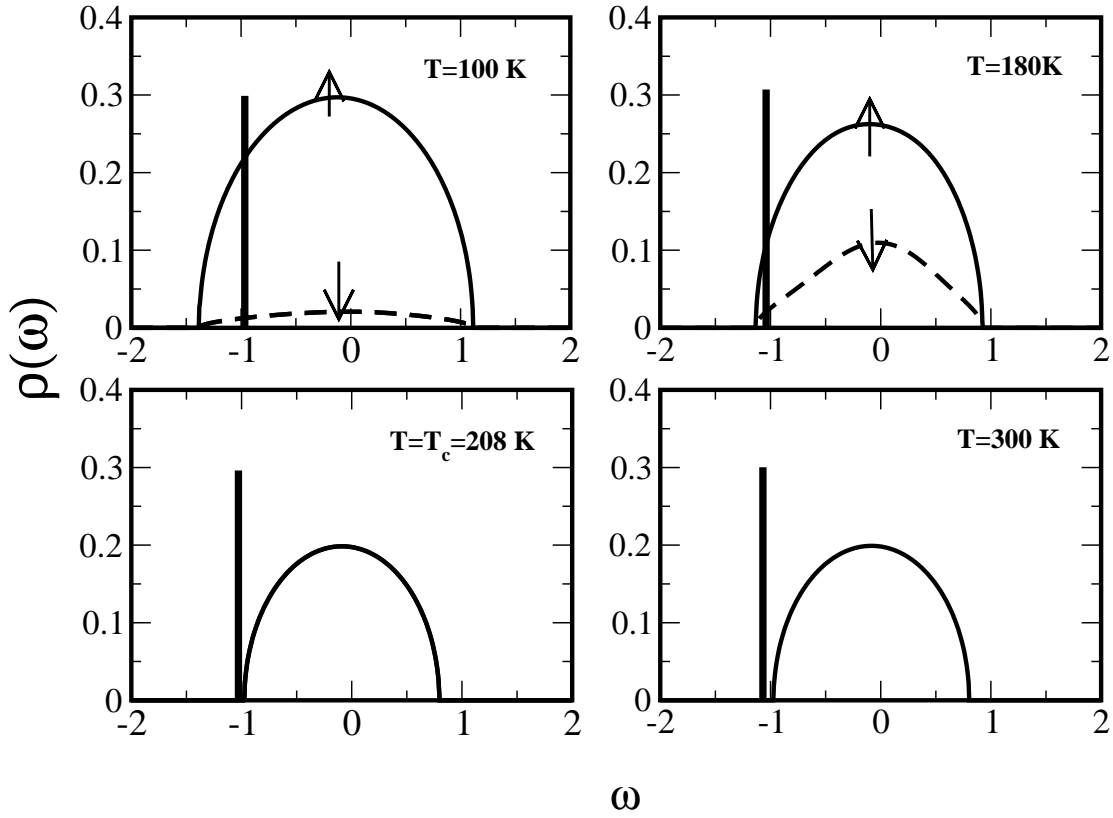


Figure 3: Evolution of the spectral function  $\rho_b(\omega)$  for parameter values that correspond to  $Sr$  doping (see text), for  $T = 100\text{K}$ ,  $180\text{K}$ ,  $208\text{K}$ ,  $300\text{K}$  and  $x = 0.175$ . Thick lines represent the effective  $\ell$  level and up and down arrow indicate up spin and down spin spectral functions.

temperature, the  $t_{2g}$  spin order decreases and the  $b$  band narrows again, since due to double exchange [39] the effective hopping amplitude of the  $b$  electrons decreases. The spectral weight for the down spin polarization also turns on, reflecting the reduction in the magnetization from its zero temperature value. The sequence of figures 3a to 3c illustrates this progression. Eventually, both up and down spin spectral functions become equal, and the  $b$  band bottom crosses the  $\ell$  level and moves up as  $T$  rises beyond  $T_c$  ( $= 208$  K in the present context, see Fig. 3c) where ferromagnetism disappears, and the system becomes a paramagnetic insulator as in Fig. 3d, with  $b$  states occupied thermally across a gap. We thus have a simple picture of the thermal ferromagnetic-metal to paramagnetic-insulator transition.

## 6 Resistivity, CMR and material systematics

There are very few calculations [20, 21, 22] of the transport properties of manganites though this is one of their main unusual features. Within the DMFT for our model, the electrical resistivity  $\rho$  can be calculated in a straightforward way [36] from the  $b$  electron propagator or Green's function. Fig. 4 shows some of our results, for  $x = 0.3$  and parameters representative of  $Nd_{1-x}Sr_xMnO_3$  and  $La_{1-x}Ca_xMnO_3$  [40]. Experimental values are also given for comparison [41].

We see that the resistivity of the paramagnetic insulating state is fairly well described by the theory. In this phase, the conducting  $b$  band is only thermally occupied. The effective electrical gap  $\simeq 850K$  (the experimental value is  $\simeq 1250K$  [41]). The positive feedback between the thermally excited, strongly  $T$  dependent number  $\bar{n}_b(T)$  of  $b$  electrons, and the double exchange broadening of the  $b$  band as  $T$  decreases, leads to a very rapid decrease and closure of the electrical gap just below  $T_c$  and the consequent rapid decrease in the resistivity just below  $T_c$  as in experiment to a rather large value  $\simeq 2 m\Omega cm$ . But we note that the calculated resistivity does not decrease much thereafter down to  $T = 0$ , unlike experiments, where  $\rho(T)$  decreases to residual values of  $\simeq 50 \mu\Omega cm$  below about  $T = 125K$ . We believe that the latter is due to inter-site  $\ell$  coherence, neglected here (see later).

We also show in the Fig. 4 the resistivity in a field of  $7Tesla$  for  $Nd_{1-x}Sr_xMnO_3$ . We clearly see CMR. The external magnetic field polarizes the  $t_{2g}$  spins, and via  $J_H$  increases the  $b$  band width which reduces the electrical gap. CMR arises because resistivity depends exponentially on the gap. The effect is largest near  $T_c$  as the change in the magnetization due to a given magnetic field is the largest there. As our mean field approximation for the Curie transition neglects short range magnetic order above  $T_c$ ,  $\rho$  is somewhat overestimated and the CMR somewhat underestimated.



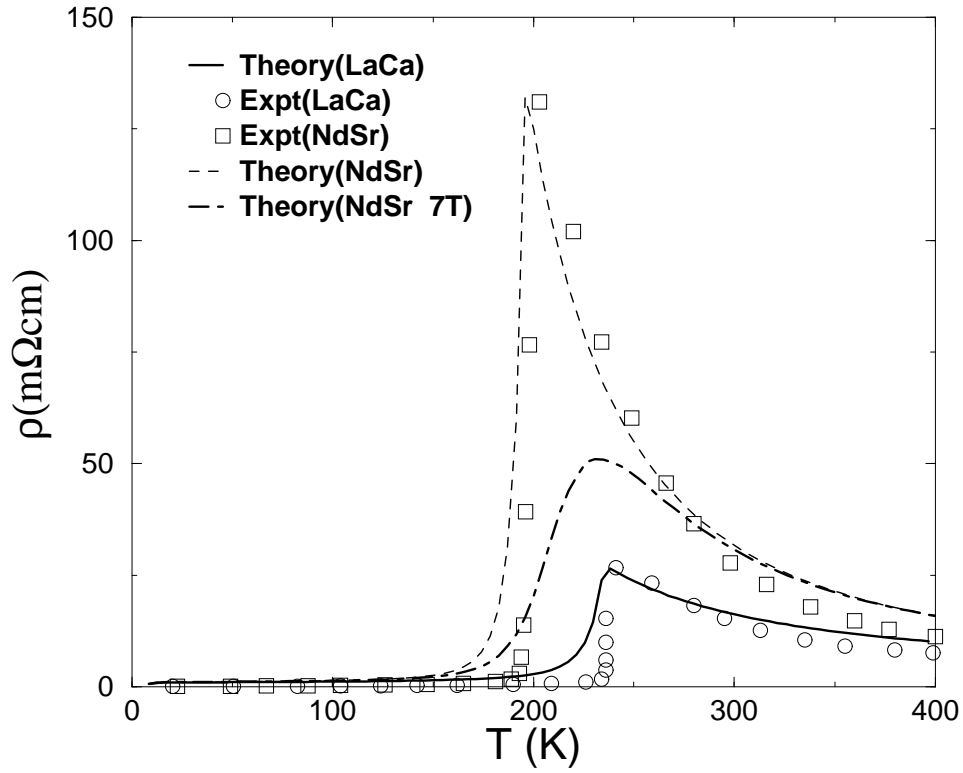


Figure 4: Electrical resistivity and CMR in the coexisting JT polaron - broad band model for  $E_{JT} = 0.5 eV$ ,  $U = 5 eV$  and  $x = 0.3$ .  $D_o$  and  $\bar{J}_F$  are chosen so as to reproduce the experimental[41]  $T_c$  and  $\rho(T_c)$  of  $Nd_{1-x}Sr_xMnO_3$  ( $D_o = 1.05 eV$ ,  $\bar{J}_F = 52.7 meV$ ) and of  $La_{1-x}Ca_xMnO_3$  ( $D_o = 1.15 eV$ ,  $\bar{J}_F = 60.2 meV$ ). Calculated  $\rho(T)$  at  $H = 7 Tesla$  is shown for  $Nd_{0.7}Sr_{0.3}MnO_3$

The properties of manganites vary strongly and characteristically with the ionic species  $Re$  and  $A$ . The material systematics of such variation, eg., in the thermal IMT as well as the CMR depend in our model largely and sensitively on the ratio ( $D_o/E_{JT}$ ) and somewhat on the  $D_o$  and  $J_F$ . A small increase in  $D_o/E_{JT}$  reduces the high temperature resistivity  $\rho(T > T_c)$  enormously, as is clear in Fig. 4 where we have increased  $D_o$  from 1.05 to 1.15 eV and  $\bar{J}_F$  from 52.7 to 60.2 meV to fit  $T_c$  and  $\rho(T_c)$  for  $La_{0.7}Ca_{0.3}MnO_3$ . Broadly this is because the density of current carrying  $b$  electrons and hence  $\sigma(T) = 1/\rho(T)$  depends exponentially on  $(E_{JT} - D_o)$ . This is also the general reason for the observed large variation of  $\rho(T > T_c)$  and  $T_c$  with strain and pressure.

Making the reasonable assumption that  $E_{JT}$ , a single octahedron quantity, is roughly unchanged across materials, but that  $\bar{J}_F$ , the effective ferromagnetic exchange, scales as  $D_o^2$ , we have calculated properties as a function of  $D_o$  for  $x \simeq 0.3$ . We find that  $T_c$  is typically fairly close to the (Curie-Weiss) value ( $\bar{J}_F/3$ ) (and hence increases as  $D_o^2$  as  $D_o$  increases), with a slight enhancement due to a nonzero  $\bar{n}_b(T_c)$  and double exchange. With increasing  $D_o$ , the resistive transition on lowering  $T$  through  $T_c$  changes from insulator-insulator to insulator-metal, and then to metal-metal. These trends are seen experimentally [6] as a function of increasing cation radius  $\langle r_A \rangle$ , which is known to roughly track the bandwidth  $D_o$ . We also find that the relative CMR, defined as  $[R(H) - R]/R(H)$ , depends exponentially on  $T_c$  (increasing as  $T_c$  decreases). This is indeed the behaviour extracted from measurements on several systems [42]. The observed unusually large dependence of  $T_c$  and of the resistivity at  $T_c$  on pressure [43] in  $La_{1-x}Ca_xMnO_3$  is reproduced if we assume that  $D_o$  increases with pressure at a realistic rate of about .01 eV/Kbar. A more detailed discussion of these finite temperature results and material trends is presented in [27].

A key feature of our theory is the result mentioned above that the dominant contribution to  $T_c$  comes from virtual double exchange of the localized  $\ell$  polarons and not from conventional double exchange, since the mobile carrier density ( $\bar{n}_b$ ) is very small. Interestingly, the precipitous, universal and nearly linear drop in  $T_c$  with local ion size variance reported by Attfield[7] in a variety of multi-component manganites is much larger than what is expected from a simple double exchange picture. In the double exchange mechanism,  $T_c$  is proportional to  $t_{ij}$  which depends on the  $Mn - O - Mn$  bond angle  $\phi_{ij}$ , which is strongly affected by the local ion-sizes, as  $\cos(\phi_{ij})$ . The variance in  $\phi_{ij}$ , namely  $\langle (\delta\phi_{ij})^2 \rangle^{1/2}$  is at most 10 degrees, so that one expects that the resulting reduction in  $T_c$  is  $\Delta T_c/T_c \sim \langle (\delta\phi_{ij})^2 \rangle / 2 \sim 1/60$ . The observed reduction is an order of magnitude larger! We believe that such a large reduction is however understandable within our theory if we extend the calculations described above to include the effect of ion size variance on  $E_{JT}$ , and

$\ell - b$  hybridization effects as discussed in section 8.

## 7 Other unusual properties

We now illustrate through three examples how other unusual properties of manganites can be understood in our approach. Specifically, we consider the anomalously low carrier density as inferred from optical conductivity in the metallic phase [44], the small electronic specific heat [4] and the electron hole asymmetry [45].

### 7.1 Low metallic carrier density

In the metallic regime ( $0.2 \lesssim x \lesssim 0.5$ ), one can estimate  $n_{eff}$ , the effective density of carriers, from the the Drude weight i.e. the frequency integral of the real part of the optical conductivity  $\sigma_r(\omega)$ . In a free electron like limit, this integral is  $(\pi n e^2 / 2 m^*)$  where  $n$  is the density of carriers, and  $m^*$  is the band optical mass. Since there is no evidence for enhancement of  $m^*$  with respect to the band mass (eg. see Ref.[4]), results for  $La_{1-x}Sr_xMnO_3$ [44] lead to  $n_{eff} = 0.06$  for  $x = 0.3$  and  $T = 0$ . The expected value (for a doped Mott insulator) is  $(1 - x) = 0.7$ . Although there are several uncertainties in inferring  $n_{eff}$  precisely from  $\sigma_r(\omega)$ , its reduction by nearly an order of magnitude, and even more so its observed strong decrease with temperature on the scale of  $T_c$  which is much less than the (normal) Fermi temperature, are puzzling. But the results are easily understood in our model, since the low frequency  $\sigma(\omega)$  is due to  $b$  electrons. As seen from Fig. (2c) at  $T = 0$  there are indeed very few electrons in the  $b$  band, all near its bottom, below the  $\ell$  (or Fermi) level. The DMFT calculation with parameters appropriate for  $La_{1-x}Sr_xMnO_3$  at  $x = 0.3$ , namely  $E_{JT} = 0.45 eV$ ,  $D_o = 1.28 eV$ ,  $\bar{J}_F = 1150 K$  (and consequently  $T_c = 390 K$ ), leads to  $\bar{n}_b(T = 0) = 0.12$ , and a decrease with temperature which is very similar to what is seen in experiment.

### 7.2 Normal linear electronic specific heat

The low  $T$  electronic specific heat in manganites (see Ref. [4] for a review) goes as  $\gamma T$  with a  $\gamma$  nearly independent of  $x$ , unlike other doped Mott insulators(eg Ref. [4]) and has a value expected for a tight binding band with bandwidth  $2D_o \simeq 2.0eV$ . In polaron theories with  $\bar{n}_\ell$  polarons per site  $C_v = \bar{n}_\ell k_B$  in the classical gas limit, and  $\sim \bar{n}_\ell k_B (k_B T / D^*)$ , where  $D^*$  is the effective bandwidth, for  $T \ll (D^* / k_B)$ . Neither of these is observed and this is often argued to be evidence against small polarons in

manganites. In our model, although the electrons are mostly JT polarons, we expect that they will make very little contribution to the low temperature specific heat. For, being localized they will strongly couple to disorder potentials and affected by coulomb interactions, and we expect that their entropy will be frozen out at a large temperature scale. We find that  $\gamma$  (calculated in the paramagnetic metallic phase to avoid large magnetic contributions to the specific heat) is about  $0.9 (mJ/K^2mole)$  with the parameters used above for  $La_{0.7}Sr_{0.3}MnO_3$ . The value for a band of width  $2 eV$  is about  $2.0 (mJ/K^2mole)$ . The physical reason for the smaller  $\gamma$  is that the few  $b$  electrons which are present occupy states near the bottom of the  $b$  band with energy close to  $-E_{JT}$ , and the density of states there is relatively smaller (Fig. 2c).

### 7.3 Electron hole asymmetry

The electronic and magnetic properties of hole doped ( $x < 0.5$ ) and "electron doped" ( $x > 0.5$ ) manganites are very different. For example, the latter are much more metallic than the former in the paramagnetic phase [45] (although the AF or charge ordered phases can be insulating for other reasons). This behaviour is unexpected in a one orbital strong coupling antiadiabatic polaron model since for low  $e_g$  carrier density the dilute small polaron assembly will form an insulator, as also in a model with only  $J_H$ , where there is electron hole symmetry. It is often stated that polaronic effects are not seen for  $e_g$  orbitals in the  $e$  doped regime because the JT coupling becomes weaker as  $x \rightarrow 1$ . This seems unlikely given the local nature of the JT interaction and the stability of the ( $MnO_6$ ) octahedron.

The metallic nature of the  $e$  doped regime which has low  $e_g$  density is natural in our theory because for large  $x$  the effectively uncorrelated  $b$  electrons form a wide band whose bottom is occupied by the small number of  $e_g$  electrons, and the  $\ell$  states are unoccupied, as depicted in Fig. 2d. This fact also explains why pure band models are fairly successful[46] in describing the magnetic ground states in the the  $e$  doped limit.

## 8 Discussion

In summary, we have presented here a new model of coexisting localized JT polarons and broad band electrons for manganites, argued that it arises inevitably in the presence of orbital degeneracy and strong JT coupling, and shown that it explains a wide variety of characteristic properties of manganites. In this concluding section we compare our theory with some of the other theories, discuss some of the inadequacies

of the present model and extensions to overcome these. We believe that a more general treatment of the model Eq. 2 with some extensions can lead to a complete description of manganites. Two examples, namely inclusion of spatial correlations and of intersite  $\ell$  state coherence are discussed below.

To begin with, we note that the picture developed here is very different from that in other polaronic models, which either neglect  $e_g$  orbital degeneracy [22, 23] or work in the adiabatic approximation [21, 47]. In the former, for example, at high temperatures transport is due to the activated hopping of localized small polarons. In the latter (adiabatic) models, the polarons also form a broad band, whence it is difficult to obtain a paramagnetic insulator to ferromagnetic metal transition say at  $x \simeq 0.3$ . Furthermore, small polarons disappear below  $T_c$  even for large  $g$ , the Drude weight is not small, and there is no isotope effect, all in disagreement with experiment. In both, it is argued that small polarons are likely only at high temperatures, and that small and large polarons coexist only in a narrow range of  $x$  and  $T$  determined by the effective electron phonon coupling and that there are no small polarons at low  $T$ .

In our theory, the carriers are broad band electrons thermally promoted out of localized JT polaronic states. Small JT polarons (in the anti-adiabatic limit, with negligible bandwidth) and band states (in the adiabatic limit) necessarily coexist over a wide range of  $x$  ( $0.2 \lesssim x \lesssim 0.7$  say) and for all  $T$ . In contrast, in single orbital polaron models, there is a crossover with increasing dimensionless electron phonon coupling  $\lambda_{eff}(x, T) = \{g^2/K W_{eff}(x, T)\}$  from large to small polarons, so that the two can occur together only over a narrow range of  $x$  and  $T$ .

*An unusual feature of the polaron level in our model is that it has no prominent thermodynamic or spectroscopic (sharp level) manifestations.* Firstly as pointed out above, it does not lead to a large electronic specific heat as we expect that their entropy will be frozen out at energy scales determined by coulomb and impurity interactions not explicitly included in our model. The remaining linear specific heat for the  $b$  band metal, is roughly of the size seen experimentally[4]. Secondly, no sharp  $\ell$  like spectral feature is to be expected. Rather, the  $\ell$  excitation spectrum will be an incoherent continuum, starting from a weak (weight  $\propto \eta \simeq 1/200$ ) anti-adiabatic low energy part building up to adiabatic (Franck-Condon) higher energy features, as the fast removal of an  $\ell$  electron leads to highly excited lattice states (energy  $\sim 2E_{JT}$ ). Indeed, optical conductivity data in manganites do show[44] such an incoherent continuum which is largely independent of temperature, and we believe that this is their origin.

In our theory presented earlier we made the simple approximation that the local

$JT$  distortion  $Q_o$  is independent of  $x$  and  $T$ , and that its large value is determined entirely by on-site properties, namely the electron  $JT$  phonon coupling  $g$  and the phonon mode force constant  $K$ . This is probably valid for high temperatures not too far below  $T_c$  and for  $x \lesssim 0.5$ . However,  $JT$  polaronic effects can become dynamical and unobservable at low  $T$  for two reasons. Firstly, the local lattice kinetic energy has a term  $(1/2)MQ_o^2\dot{\theta}_i^2$  where  $Q_o$  is the magnitude, and  $\theta_i$  the direction or orientation, of the local  $JT$  distortion. Hence  $\theta_i$ , which also determines the orbital mixing amplitudes of the  $\ell$  and  $b$  states, rotates due to quantum fluctuations, although due to anharmonicity and crystallinity, the rotation could be hindered and slow. A second, perhaps more important, source of this dynamical  $J - T$  effect is the quantum mechanical intersite  $\ell$  state coherence which makes the  $\theta_i$  ill defined. The energy scale for the latter,  $D^* \sim 125K$ , is consistent with the widely observed [4, 9, 11, 13] reduction or disappearance of static or of long time scale local  $JT$  distortion in metallic manganites as their temperature decreases well below 125K. Finally, intersite  $\ell$  coherence, especially hybridization with energetically degenerate broad band  $b$  states in the metallic regime, will reduce  $Q_o$  and broaden the  $\ell$  band. The two effects feed back on each other, and it is in principle possible that small polarons may weaken and disappear altogether at low temperatures in the metallic phase rather than merely becoming dynamic. We have not explored this possibility here.

Intersite  $\ell$  state coherence can be included in our model by adding to Eq.(1) an  $\ell - b$  hybridization term  $\sum_{\langle ij \rangle, \sigma} [t_1(\ell_{i\sigma}^+ b_{j\sigma} + b_{j\sigma}^+ \ell_{i\sigma}) + t_2 \ell_{i\sigma}^+ \ell_{j\sigma}]$  where  $t_1 \sim \bar{t}\eta \sim D^*$ , and  $t_2 \sim \bar{t}\eta^2$ . We expect that its inclusion, and the consequent development of long range intersite  $\ell$  state coherence at low temperatures will, in addition, lead to the observed smooth decrease [19] in the electrical resistivity of clean metallic manganites from about  $1 m\Omega cm$  just below  $T_c$  to a small value,  $\simeq 50 - 100 \mu\Omega cm$ , as  $T \rightarrow 0$  past a characteristic crossover temperature of about 100K, of the same scale as  $D^*$ . In the DMFT calculations presented above, the residual resistivity at  $T = 0$  due to random scattering from the incoherent  $\ell$  sites is too large,  $\sim 1 m\Omega cm$  (Fig.3). If the  $\ell$  states become coherent, the  $b$  electron scattering and the consequent resistivity would then vanish at  $T = 0$ , and is nonzero only if static disorder is present. This can lead to a metallic state with a small residual resistivity or to an Anderson localized insulating state depending on the amount of disorder.

We believe that the giant isotope effect observed in manganites [19] is another dramatic consequence of the  $\ell - b$  hybridization scale  $t_1$  and its exponential dependence on the inverse square root of the isotopic mass. For it can add, via (conventional) double exchange, to the ferromagnetic  $T_c$  an amount roughly given by  $\Delta T_c \simeq \alpha \bar{n}_\ell (D^*/k_B) \simeq (87\alpha) K$  for  $\bar{n}_\ell = 0.7$  where  $\alpha$  is less than one. Because of the

Huang Rhys factor in  $D^*$ , which depends exponentially on square root of the isotopic mass, we find that  $\Delta T_c(O^{16}) \simeq (1.33) \Delta T_c(O^{18})$  so that for  $\alpha \simeq (1/2)$  the difference  $T_c(O^{16}) - T_c(O^{18}) \sim 15 K$ , close to the observed value[19].

In addition to the neglect of intersite coherence effects discussed above, we have also neglected in our theory spatial correlations between the local electron densities  $n_{\ell i}$  and  $n_{bi}$ , as well as between the local angles  $\theta_i$ . This may be adequate for the phases which correspond to *homogenous orbital liquids*. However, many phenomena in manganites such as short range order, long range charge/orbital order (or *orbital solidification*), various types of antiferromagnetism [3, 4] and mesoscale structures [6] depend on spatial correlations. To treat these we need to add to eq. (1) a number of more complicated longer range coulomb, anharmonic, steric, elastic, magneto-elastic, etc. interactions that couple spin, orbital and lattice degrees of freedom to each other, and to strain, ion size mismatch, disorder, etc. as appropriate. A self consistent determination of long or short range order in  $\delta_i \equiv (\bar{n}_{\ell i} - \bar{n}_{bi})$  (a new ‘internal’ variable)[48],  $\theta_i$  and  $\vec{S}_i$ , and their effects on the  $b$  electron dynamics for different  $x$  and  $T$ , in the presence of such interactions can lead to a complete description of manganites including the above phenomena, and others such as first order transitions, two phase co-existence, etc.. We hope to discuss these elsewhere.

A significant general question raised by our work is that of the detailed nature of adiabatic to non adiabatic crossover as  $g$  increases, and the conditions for the *coexistence of adiabatic and antiadiabatic states with exponentially separated dynamical timescales*. We have shown that the latter leads to new phenomena, argued that this happens in manganites because of the large  $g$ , and have developed the consequences in a simple model assuming this separation. The results closely correspond with a wide variety of observations. It would be of great interest to explore such a crossover and time-scale or energy-scale separation experimentally and theoretically in the many systems such as organic solids, transition metal oxides and chemical (molecular) systems, which have degenerate orbitals and strong symmetry breaking JT couplings.

We would like to acknowledge support from several agencies. HRK has been supported in part by grant no. 2404-1 of the Indo French Centre for Promoting Advanced Research, TVR in part by a US-India project ONR N 00014-97-0988, and SRH and GVP in part by the Council of Scientific and Industrial Research, India.

## References

- [1] See for example, P. W. Anderson, *The Theory of Superconductivity in the High- $T_c$  Cuprates* (Princeton Univ. Press, Princeton, 1997).
- [2] S. Jin, et al. *Science* **264**, 413 (1994).
- [3] Y. Tokura, ed. *Colossal Magnetoresistance Oxides*(Gordon and Breach, New York, 2000).
- [4] M. B. Salamon, and M. Jaime, *Rev. Mod. Phys.* **73**, 583 (2001).
- [5] N. D. Mathur and P. B. Littlewood, *Solid State Communications* **119**, 271 (2001).
- [6] These could arise from the mismatch of *Re* and *A* ion size with respect to the value for the ideal close packed  $ABO_3$  structure, see for example: H. Y. Hwang, et. al. *Phys. Rev. Lett.* **75**, 914 (1995).
- [7] J. P. Attfield, *Chemistry of Materials* **10**, 3239 (1998).
- [8] N. A. Babushkina, et al, *Nature* **391**, 159 (1998).
- [9] E. Dagotto, T. Hotta, and A. Moreo, *Physics Reports.* **344**, 1 (2001). See also, E. Dagotto, *Nanoscale Phase Separation and Colossal Magnetoresistance* (Springer, Berlin, 2002)
- [10] M. Uehara, S. Mori, C. M. Chen, and S. W. Cheong, *Nature* **399**, 560 (1999).
- [11] D. Louca, et al., *Phys. Rev. B.* **56**, R8475 (1997); T. Egami in *Structure and Bonding* (ed. J. B. Goodenough) vol. 98, p115 (2001)
- [12] C Meneghini, et al, *J Phys. Cond. Mat.* **14**, 1967 (2002).
- [13] R. H. Heffner, et. al. *Phys. Rev. Lett.* **85**, 3285 (2000).
- [14] M. Fäth, et al. *Science* **285**, 1540 (1999).
- [15] S. Satpathy, Z. S. Popovic and F. R. Vukajlovic, *Phys. Rev. Lett.* **76**, 960 (1996).
- [16] D. D. Sarma, et. al. *Phys. Rev. Lett.* **75**, 1126 (1995).
- [17] A. J. Millis, *Phil. Trans. R. Soc. Lond. A* **356**, 1473 (1998).



- [18] Large JT splitting is the traditional basis of our understanding of  $LaMnO_3$  structure, see eg J. Kanamori, *J. Appl. Phys.* **31**, 14S (1960).
- [19] G. M. Zhao, et. al. *Phys. Rev. B* **63**, 060402 (2001).
- [20] N. Furukawa, *Journal of the Physical society of Japan* **64**, 2734 (1995).
- [21] A. J. Millis, R. Mueller, and B. I. Shraiman, *Phys. Rev. B* **54**, 5405 (1996).
- [22] A. C. M. Green and D. M. Edwards, *Jl. Magn. Magn. Mater.* **226**, 886 (2001).
- [23] H. Roder, Jun Zang, and A. R. Bishop, *Phys. Rev. Lett.* **76**, 1356 (1996).
- [24] M. Uehara, K. H. Kim and S. W. Cheong, private communication.
- [25] N. M. Iliev and V. M. Abrashev, *J. Raman Spectrosc.* **32**, 805 (2001)
- [26] K. Huang and F. Rhys, *Proc. Roy. Soc. London Ser. A* **204**, 406 (1950)
- [27] T. V. Ramakrishnan, H. R. Krishnamurthy, S. R. Hassan and G. V. Pai cond-matt/0308376, *submitted for publication*
- [28] G. Venketeswera Pai, S. R. Hassan, H. R. Krishnamurthy and T. V. Ramakrishnan *submitted for publication*
- [29] The relatively small  $g\mu_B\vec{H} \cdot \vec{s}_i$  term in  $H_s$  and other coulomb repulsion terms in  $H_{\ell b}$  have been neglected because of the large  $J_H$  ( $J_H \gg \bar{t}$ ) limit, of relevance here.
- [30] For a discussion of such vibronic states with JT coupling, see M. D. Sturge, in *Solid State Physics* (Eds. F. Sietz, D. Turnbull and H. Ehrenreich, Academic Press, New York.) **20**, 91 (1967).
- [31] G. I. Lang and A. Yu. Firsov, *Soviet Physics JETP* **43**, 1843 (1962).
- [32] eg., see T. V. Ramakrishnan and G. V. Pai, *Jl. Low Temp. Phys.* **126**, 1055 (2002) for a discussion of such issues in a simpler one orbital spinless polaron model.
- [33] In the limit that this amplitude is zero, we have two classical regions, one with small polarons and another with broad band states; this is the percolative regime discussed in the literature (eg. [9, 10]).

- [34] T. Mizokawa, D. I. Khomskii and G. A. Sawatzky, *Phys. Rev. B* **63**, 024403 (2001); See also A. J. Millis, *Phys. Rev. B* **55**, 6405 (1997)
- [35] L. M. Falicov and J. C. Kimball, *Phys. Rev. Lett.* **22**, 997 (1969).
- [36] A. Georges, G. Kotliar, W. Krauth and M. J. Rozenberg, *Rev. Mod. Phys.* **68**, 13 (1996).
- [37] We note that the approach of Millis, Muller and Shraiman [21] which we have commented on earlier is similar, except that they set  $U = 0$  and treat the JT distortions purely classically.
- [38] S. R. Hassan, *Dynamical mean-field theory of Falicov-Kimball and Related Models and their application to CMR Phenomena in Manganites*, Ph. D. Thesis (Indian Institute of Science, Bangalore) 2003 (unpublished).
- [39] P. W. Anderson and H. Hasegawa, *Phys. Rev.* **100**, 675 (1955).
- [40] We choose  $E_{JT} = 0.5 eV$  and  $U = 5.0 eV$ , for both the systems.  $D_o$  is  $1.05 eV$  and  $1.15 eV$ , and  $\bar{J}_F$  is  $52.7 meV$  and  $60.2 meV$  respectively. These choices are made such that the observed  $T_c$  as well as  $\rho(T_c)$  are reproduced. The electrical activation energies above  $T_c$ ,  $\Delta_{theory} = 850 K, 550 K$ , are in reasonable agreement with  $\Delta_{expt} = 1250 K, 770 K$  respectively. Further the steep drop in  $\rho$  below  $T_c$  is well reproduced.
- [41] P. Dai, et. al. *Phys. Rev. B* **61**, 9553 (2000).
- [42] K. Khazeni et. al. *Phys. Rev. Lett.* **76**, 295 (1996).
- [43] J. J. Neumeier, M. F. Hundley, J. D. Thompson and R. H. Heffner *Phys. Rev. B* **52**, R7006 (1995).
- [44] Y. Okimoto, et.al. *Phys. Rev. B* **55**, 4206 (1997).
- [45] A. Maignan, C. Martin, F. Damay and B. Raveau, *Phys. Rev. B* **58**, 2758 (1998).
- [46] G. V. Pai, *Phys. Rev. B* **63**, 064431 (2001)
- [47] M. S. Laad, L. Craco and E. Muller-Hartmann, *Phys. Rev. B* **63**, 214419 (2001).
- [48] Variations in the local charge density  $q_i \equiv (\bar{n}_{\ell i} + \bar{n}_{b i})$  are likely to be small and of short range because of the large Coulomb energy cost. (A coulomb energy term needs to be added to Eq. 2 to describe this).